Published in final edited form as:
Cardiovasc Intervent Radiol. 2014 October ; 37(5): 1343–1351. doi:10.1007/s00270-013-0828-3.

Role for Putative Hepatocellular Carcinoma Stem Cell Subpopulations in Biological Response to Incomplete Thermal Ablation: In Vitro and In Vivo Pilot Study

Scott M. Thompson,
Medical Scientist Training Program, College of Medicine, Mayo Clinic, 200 First Street Southwest, Rochester, MN 55905, USA

Matthew R. Callstrom,
Department of Radiology, College of Medicine, Mayo Clinic, 200 First Street Southwest, Rochester, MN 55905, USA

Kim A. Butters,
Department of Radiology, College of Medicine, Mayo Clinic, 200 First Street Southwest, Rochester, MN 55905, USA

Shari L. Sutor,
Genomics Research Center, College of Medicine, Mayo Clinic, 200 First Street Southwest, Rochester, MN 55905, USA

Bruce Knudsen,
Department of Laboratory Medicine and Pathology, College of Medicine, Mayo Clinic, 200 First Street Southwest, Rochester, MN 55905, USA

Joseph P. Grande,
Department of Laboratory Medicine and Pathology, College of Medicine, Mayo Clinic, 200 First Street Southwest, Rochester, MN 55905, USA

Lewis R. Roberts, and
Division of Gastroenterology and Hepatology, College of Medicine, Mayo Clinic, 200 First Street Southwest, Rochester, MN 55905, USA

David A. Woodrum
Department of Radiology, College of Medicine, Mayo Clinic, 200 First Street Southwest, Rochester, MN 55905, USA

Scott M. Thompson: thompson.scott@mayo.edu; Matthew R. Callstrom: callstrom.matthew@mayo.edu; Kim A. Butters: butters.kim@mayo.edu; Shari L. Sutor: sutor.shari@mayo.edu; Bruce Knudsen: Knudsen.bruce@mayo.edu; Joseph P.

Correspondence to: Scott M. Thompson, thompson.scott@mayo.edu.

Conflict of interest Mr. Scott Thompson received a research grant from the SIR Foundation—Allied Scientist Training Grant. Dr. Lewis Roberts received research grants from Bristol Myers-Squibb, Merck, Nordion, and Bayer. Dr. Matthew Callstrom, Ms. Kim Butters, Ms. Shari Sutor, Mr. Bruce Knudsen, Dr. Joseph Grande, and Dr. David Woodrum declare that they have no conflict of interest.

Grande: grande.joseph@mayo.edu; Lewis R. Roberts: Roberts.lewis@mayo.edu; David A. Woodrum: woodrum.david@mayo.edu

Abstract

Purpose—To investigate the potential role for $CD44^+$ and $CD90^+$ hepatocellular carcinoma (HCC) cellular subpopulations in biological response to thermal ablation-induced heat stress.

Methods—This study was approved by the institutional animal care committee. The N1S1 rat HCC cell line was subjected to sublethal heat stress (45 °C) or control (37 °C) for 10 min, costained with fluorescent-labeled antibodies against CD44, CD90, and 7-AAD after a 48-h recovery and analyzed by flow cytometry to assess the percentage of live $CD44^+$ and $CD90^+$ HCC cells ($n = 4$). Experiments were repeated with pretreatment of N1S1 cells with a dose titration of the dual PI3K-mTOR inhibitor BEZ235 or vehicle control ($n = 3$). Rats bearing orthotopic N1S1 tumors were subjected to ultrasound-guided partial laser ablation ($n = 5$) or sham ablation ($n = 3$), euthanized 24 h after ablation, and liver/tumor analyzed for immunohisto-chemical staining of CD44 and CD90. Differences between groups were compared with an unpaired *t* test.

Results—Sublethal heat stress induced a significant increase in the relative proportion of live $CD44^+$ and $CD90^+$ HCC cells compared to the control group: $CD44^+$ $CD90^-$ (5.3-fold; $p = 0.0001$), $CD44^-CD90^+$ (2.4-fold; $p = 0.003$), and $CD44^+$ $CD90^+$ (22.0-fold; $p < 0.03$). Inhibition of PI3K-mTOR prevented heat stress-induced enrichment of the population of live $CD44^+$ HCC cells ($p < 0.01$), but not $CD90^+$ cells ($p > 0.10$). Immunohistochemical analysis demonstrated preferential localization of clusters of $CD44^+$ cells at both the tumor margin and ablation margin.

Conclusion—These studies provide experimental evidence supporting a role for HCC cells expressing the putative stem cell marker CD44 in HCC response to heat stress.

Keywords

Hepatocellular carcinoma; Cancer stem cell; Thermal ablation; CD44

Introduction

Stem cells are present in many tissues and play an important role in normal tissue physiology and homeostasis [1]. Although stem cells play a key role in normal tissue homeostasis, studies over the past 30 years have demonstrated that stem cell-like cells may play a key role in oncogenesis [2, 3]. Relatively rare subpopulations of malignant cells with stem cell-like features have been isolated from both hematopoietic and solid organ malignancies, resulting in development of the cancer stem cell (CSC) hypothesis [1, 3, 4]. The CSC hypothesis holds that mutations in normal stem or progenitor cells give rise to CSC with the capacity to initiate and sustain tumor growth; they have been implicated in tumor metastasis and resistance to anticancer therapies [1, 4–6]. For example, it is hypothesized that tumor recurrence after initial treatment response with cytotoxic chemotherapy results from preferential killing of differentiated cancer cells while residual CSC can repopulate the tumor [1]. As such, efforts are underway to better understand the cytoprotective mechanisms of CSC in order to identify therapeutic targets for enhancing the killing of CSC with anticancer treatments [7, 8].

In hepatocellular carcinoma (HCC), subpopulations of HCC cells that have stem cell-like properties have been isolated from both primary tumors and immortalized cell lines by their differential expression of cell surface cluster differentiation (CD) markers [9]. Currently recognized putative HCC CSC markers include CD13, CD44, CD90 (Thy-1), CD133, and CD326 (EpCAM) [9–19]. CSC from various malignancies including HCC have been shown to be regulated by diverse oncogenic pathways such as the PI3K-AKT-mTOR signaling, a critical cell survival mechanism [20–32]. In HCC, a previous study demonstrated that HCC CSC were more chemoresistant to doxorubicin as a result of up-regulation of AKT-mediated survival signaling [13].

Percutaneous thermal ablative therapies have greatly expanded treatment options for nontransplantable HCC patients while achieving short-term outcomes similar to surgical resection with less morbidity [33–36]. However, as tumor size increases, thermal ablation of HCC has increasing rates of local recurrence and tumor progression, particularly for tumors beyond 3 cm in size, and overall survival remains poor for these patients [34, 37–40]. As such, there remains a need to identify potential biological mechanisms mediating HCC response to thermal ablation. However, it is not known whether putative CSC may play a role in HCC response to heat stress from thermal ablative therapies. The aim of the present study was to investigate the potential role for $CD44^+$ and $CD90^+$ HCC cellular subpopulations in biological response to thermal ablation induced heat stress

Methods

Cell Lines

The N1S1 (ATCC, Manassas, VA) and AS30D (DSMZ, Braunschweig, Germany) rat HCC cell lines were cultured according to supplier recommendations.

Materials

Reagents—NVP-BEZ235 was purchased from Selleck Chemicals; 7-AAD (#559925) was purchased from BD Biosciences.

Antibodies—For flow cytometry, PE Mouse Anti-CD13 (#560998), FITC Mouse Anti-Rat CD44H (#550974), APC Mouse Anti-Rat CD90 (#561409), PE Anti-EpCAM, CD326 (#347198), FITC Mouse IgG2a, κ Isotype Control (#553456), APC Mouse IgG1, κ Isotype Control (#550854), and PE Mouse IgG1, κ Isotype Control (#555749) antibodies were purchased from BD Biosciences.

Immunohistochemistry—Rat anti-CD44 polyclonal antibody (#251174) and rat anti-CD90 (Thy-1) polyclonal antibody (#251285) were purchased from Abbiotec.

In Vitro Heat Stress Protocol—To determine in vitro sublethal heat stress conditions that induce a significant reduction in cell survival at 48 h after heat stress but still result in some viable HCC cells, N1S1 and AS30D cells were suspended in complete media in 1.5 ml microcentrifuge tubes and heat stressed at temperatures from 37 to 60 °C for 10 min in an isothermic water bath. Treatment temperature was monitored with an Omega HH41 digital thermometer (Omega Engineering, Stamford, CT) and maintained to within ±0.05 °C. Cells

were then plated in 96-well tissue culture plates and incubated in a 37 °C, 5 % CO_2 incubator. At 48 h after heat stress, a WST-1 viability assay (Roche, Manheim, Germany) was performed per the manufacturer's instructions. Absorbance was measured on a DTX 880 microplate reader (Beckman Coulter). Absorbance data were normalized to the non-heat stressed (37 °C) control to determine relative cell viability and plotted versus temperature. Nonlinear regression curve fitting was used to calculate a heat stress IT_{50} by Prism 5.0 (GraphPad Software, Inc., La Jolla, CA). IT_{50} was defined as the temperature that induced a 50 % reduction in cell viability relative to 37 °C control for a 10-min exposure time. The experimental conditions based on the IT_{50} data were used to recapitulate an incomplete thermal ablation in vitro for subsequent experiments.

For heat stress only experiments, N1S1 cells were heat stressed (45 °C) or control (37 °C) for 10 min in an isothermic water bath (n = 4 independent N1S1 cell cultures). For combination drug-heat stress experiments, N1S1 cells were pretreated with a dose titration of NVP-BEZ235 (0.02, 0.1, or 0.5 μM) or vehicle control (0.1 % DMSO) for 1 h followed by sublethal heat stress (45 °C) or control (37 °C) for 10 min (n = 3 independent N1S1 cell cultures). Cells were recovered in complete media in a 37 °C, 5 % CO_2 humidified incubator for 48 h followed by analysis by fluorescence activating cell sorting (FACS). N1S1 cells were gated on the live cell population (7-AAD negative), and the percentage of $CD44^+$ $CD90^-$, $CD44^-CD90^+$, and $CD44^+$ $CD90^+$ cells from the live cell population was determined by dividing the number of positive cells by the total number of cells in the parent population.

Stem Cell Marker-Based Flow Cytometry—For initial screening of HCC stem cell markers, N1S1 and AS30D cells were rinsed in 1× PBS and stained with fluorescent-labeled antibodies against CD13, CD44, CD90, CD326, or corresponding isotype controls for 30 min on ice protected from light (n = 3 independent cell cultures). Cells were then rinsed with ice-cold 1× PBS and resuspended in phenol-red free complete media to a final concentration of 1×10^6 cells/ml. For heat stress experiments, N1S1 cells were rinsed in 1× PBS and costained with fluorescent-labeled antibodies against CD44 and CD90 or corresponding isotype controls for 30 min on ice protected from light. Cells were then rinsed with ice-cold 1× PBS, stained with the live–dead cell stain 7-AAD for 10 min, and resuspended in phenol-red free complete media to a final concentration of 1×10^6 cells/ml. All cells were analyzed with a FACSCanto digital flow cytometer (BD Biosciences). Gating parameters were adjusted according to negative and positive single-stain controls. Data were analyzed by BD CellQuest Pro software (BD Biosciences).

Animal Model—All studies were approved by the institutional animal care and use committee (IACUC). The N1S1 orthotopic HCC model was developed as previously described (n = 8) [41]. Rats were randomized to ultrasound (US)-guided partial laser ablation (n = 5) or sham laser ablation (n = 3) using methods previously described [41]. Briefly, all ablation experiments were performed using an US Food and Drug Administration-approved 980-nm laser generator (Visualase, Houston, TX). Under ultrasound guidance with an L8-18i transducer (logiq E9 Ultrasound, GE Healthcare), a bare 400-μm core optical laser fiber with a 1.0-cm diffusing tip was percutaneously inserted

through a 22-gauge introducer sheath at the tumor margin, and a 22-gauge needle with a 25-gauge wire thermocouple (Valleylab, Boulder, CO) was inserted 4–5 mm from the laser fiber tip within the tumor for intraprocedural temperature monitoring. For the ablation group, tumors were ablated at a power setting of 3 W under continuous US monitoring, and the ablation stopped when the thermocouple reached 45 °C in order to generate an intentional partial ablation. The laser was not turned on for sham-ablated animals. Rats were euthanized by CO_2 inhalation 24 h after laser or sham ablation.

Immunohistochemistry

Liver/tumor tissue was removed, and 2-mm cross sections were cut encompassing tumor and background liver. All liver/ tumor specimens were placed in 10 % neutral buffered formalin, embedded in paraffin, and sectioned with a microtome for histopathologic and immunohistochemical analysis. Paraffin-embedded sections were stained with antibodies against CD44 (1:250) or CD90 (1:100) using methods previously described [42]. All sections were reviewed by an experienced pathologist (>20 years) in a blinded and random fashion to assess tumor/liver immunostaining [42]. Digital images were captured with a Leica DMLB microscope (Leica Microsystems) equipped with a MicroPublisher 3.3 RTV camera (Q-Imaging, Surrey, BC) and the MetaVue Imaging System (v.6.3r2; Universal Imaging Corp., Downington, PA).

Statistical Analysis

Statistical analyses were performed by Prism 5.0 (GraphPad Software Inc., La Jolla, CA). Differences between groups of live $CD44^+$ $CD90^-$, $CD44^-CD90^+$, and $CD44^+$ $CD90^+$ N1S1 HCC cells were compared with an unpaired *t* test or one-way analysis of variance followed by post-hoc pairwise comparison by unpaired *t* test (or exact Mann–Whitney test). $p < 0.05$ was considered statistically significant.

Results

Heat Stress Dose–Response

Analysis of heat stress dose–response curves 48 h after heat stress showed a 50 % reduction in HCC cell viability (IT_{50}) at 45.6 °C for N1S1 (Fig. 1A) and 44.4 °C for AS30D (Fig. 1B) HCC cell lines for a 10-min heat stress exposure time. On the basis of the IT_{50} data, 45.0 °C for 10 min was chosen for subsequent experiments to recapitulate an incomplete thermal ablation in vitro.

Subpopulations of N1S1 HCC Cells are $CD44^+$ and $CD90^+$ Positive

Flow cytometric analysis identified $CD44^+$ and $CD90^+$ cells in the N1S1 cell line but not the AS30D cell line. There were no cells staining positive for CD13 or CD326 in either cell line. The mean ± SEM for the percentage N1S1 cells positive for CD44 and CD90 out of the total cell population was 0.12 ± 0.03 % and 0.15 ± 0.02 %, respectively ($n = 3$). These data demonstrate that sub-populations of rare $CD44^+$ and $CD90^+$ cells exist within the N1S1 cell line at a frequency of ~7–18 per 10,000 cells (CD44) and 9–20 per 10,000 cells (CD90).

Sublethal Heat Stress Enriches the Population of Live CD44$^+$ and CD90$^+$ N1S1 HCC Cells In Vitro

In order to determine whether sublethal heat stress enriches the proportion of live HCC subpopulations expressing putative HCC stem cell markers in vitro, sublethal heat stress of N1S1 cells followed by flow cytometric analysis for CD44 and CD90 expression at 48 h after heat stress was performed. Flow cytometric analysis showed that sublethal heat stress induced a small but significant increase in the relative proportion (% ± SEM) of live CD44$^+$ and CD90$^+$ cells compared to the 37 °C control group, as evidenced by the enrichment of CD44$^+$ CD90$^-$ (5.3-fold, 0.16 ± 0.004 % vs. 0.03 ± 0.01 %, respectively, $p = 0.0001$), CD44$^-$CD90$^+$ (2.4-fold, 0.12 ± 0.007 % vs. 0.05 ± 0.01 %, respectively, $p = 0.003$), and CD44$^+$ CD90$^+$ (22.0-fold, 13.2×10^{-6} % ± 4.3×10^{-6} % vs. 0.6×10^{-6} % ± 0.6×10^{-6} %, respectively, $p < 0.03$) subpopulations (Fig. 2). These data demonstrate that the populations of CD44$^+$ and CD90$^+$ N1S1 HCC cells, although rare, are enriched by sublethal heat stress.

Inhibition of PI3K-mTOR Prevents the Enrichment of live CD44$^+$ N1S1 HCC Cells by Sublethal Heat Stress In Vitro

In order to determine whether inhibition of the PI3K-AKT-mTOR pathway prevents the enrichment of live HCC subpopulations expressing putative HCC stem cell markers after sublethal heat stress in vitro, pretreatment of N1S1 cells with a dose titration of the dual PI3K-mTOR inhibitor NVP-BEZ235 followed by sublethal heat stress and flow cytometric analysis for CD44 and CD90 expression at 48 h after heat stress was performed. Treatment with PI3K-mTOR inhibitor at 0.1 and 0.5 μM prevented heat stress-induced enrichment of the population of live CD44$^+$ N1S1 cells ($p < 0.01$) but did not significantly prevent the enrichment of the population of live CD90$^+$ N1S1 cells ($p > 0.10$) (Fig. 3).

CD44$^+$ N1S1 HCC Cells Preferentially Localize to the Tumor Margin In Vivo

Finally, in order to determine the localization of HCC subpopulations expressing putative stem cell markers in HCC tumors in vivo, immunohistochemical staining of paraffin-embedded sections from N1S1 tumors orthotopically implanted in the livers of immunocompetent Sprague Dawley rats was performed. Immunohistochemical analysis demonstrated preferential localization of CD44$^+$ cells at the tumor margin (Fig. 4). There was no evidence of cells staining positive for CD44$^+$ in the background liver. Immunohistochemical staining for CD90 did not detect any positively staining cells in the tumor or liver (data not shown). Finally, CD44 immunohistochemical staining of N1S1 tumors that had undergone intentional partial laser thermal ablation demonstrated clusters of CD44$^+$ cells near the tumor ablation margin (Fig. 5).

Discussion

CSC have been implicated in resistance to various anti-cancer therapies, including cytotoxic and molecular-targeted agents and ionizing radiation, but have yet to be examined in the context of thermal ablation [1, 13]. These proof-of-concept studies provide experimental evidence supporting a role for HCC cells expressing putative CSC makers CD44 and CD90 in HCC biological response to heat stress.

The initial screen identified CD44- and CD90-positive cells in the N1S1 cell line but not the AS30D cell line. These findings are consistent with previous studies that have demonstrated that HCC cell lines, primary HCC tumors, and blood samples from HCC patients harbor rare subpopulations of cells expressing putative CSC markers in a patient-, tumor-, cell line-, and marker-dependent manner [9–24]. The findings that the AS30D cells do not express any of the putative CSC markers tested is consistent with the absence of these markers in other cell lines. Nonetheless, this does not rule out the possibility of other CSC markers, such as CD133 [14]. Specifically, the percentage of CD44 and CD90 cells out of the total N1S1 cell population was ~0.12 and 0.15 %, respectively, findings consistent with other studies reporting a range of 0.07–3.29 % for $CD44^+$ HCC cells and 0.02–0.19 % for $CD90^+$ HCC cells [12, 18]. A pioneering study by Yang et al. [12] demonstrated that $CD90^+$ but not $CD90^-$ HCC cells were strongly tumorigenic in immunodeficient mice and that $CD44^+$ cells developed tumors more quickly than $CD44^-$ cells. Moreover, they found that $CD44^+$ $CD90^+$ HCC cells demonstrated a more aggressive, metastatic phenotype compared to the $CD44^-CD90^+$ cells and that inhibition of CD44 using a neutralizing antibody prevented local and metastatic tumor formation by $CD90^+$ cells [12]. In short, these findings support a role for $CD44^+$ and $CD90^+$ cells in HCC tumor progression and biological heterogeneity and suggest that CD44 may represent a potential therapeutic target.

Previous studies have suggested a model whereby CSC are enriched after treatment with cytotoxic therapies, thereby promoting tumor repopulation and progression [1]. In these experiments, sublethal heat stress enriched the population of live $CD44^+$ 90^-, $CD44^-CD90^+$, and $CD44^+$ $CD90^+$ cells, although the double positive cells were extremely rare. These data support at least two potential hypotheses. First, sublethal heat stress selects for $CD44^+$ and $CD90^+$ cells, effectively decreasing the total HCC cell population while the absolute number of $CD44^+$ and/or $CD90^+$ cells does not change. This hypothesis would suggest that $CD44^+$ and/or $CD90^+$ cells are more resistant to heat stress than $CD44^-$ and $CD90^-$ cells. Second, sublethal heat stress may induce an increase in the absolute number of $CD44^+$ and $CD90^+$ cells and a decrease in the total HCC cell population. This hypothesis would suggest that sublethal heat stress induces the proliferation of $CD44^+$ and/or $CD90^+$ cells. Regardless of the mechanism, these data demonstrate that the populations of $CD44^+$ and $CD90^+$ N1S1 HCC cells, although rare, are enriched by sublethal heat stress. Given the enhanced capacity for tumor initiation, self-renewal, pluripotency, and chemoresistance in CSC, these findings may suggest that residual $CD44^+$ and/or $CD90^+$ cells promote tumor repopulation and progression after sublethal heat stress.

Diverse signaling pathways and regulatory mechanisms have been implicated in promoting the survival of CSC to anticancer therapies in HCC and other malignances [17, 43–45]. Previous studies have demonstrated that PI3K-AKT-mTOR signaling may play an important role in the enhanced survival of CSC to chemotherapy and ionizing radiation [13, 17, 25–29]. Interestingly, PI3K-mTOR inhibition prevented heat stress-induced enrichment of the population of live $CD44^+$ N1S1 cells but not $CD90^+$ N1S1 cells. These data demonstrate that PI3K-AKT-mTOR signaling may play different roles in $CD44^+$ and $CD90^+$ cells, suggesting further biological heterogeneity within the N1S1 cell line. Moreover, these data suggest that PI3K-mTOR may be a potential therapeutic target in these cell subpopulations, findings consistent with previous studies in HCC and other malignancies [13, 25].

Finally, the presence of $CD44^+$ and $CD90^+$ cells was investigated in orthotopic N1S1 tumors in vivo [33]. Interestingly, cells staining positive for CD44 were rare and preferentially localized within the N1S1 tumor at the tumor margin. Additionally, rare $CD44^+$ cells were found at the tumor ablation margin. On the other hand, cells staining positive for CD90 were not identified in the N1S1 tumor or background liver. However, the presence of $CD90^+$ cells in the N1S1 cell line in vitro but not when orthotopically implanted in vivo suggests that there may be a technical issue with the anti-CD90 antibody, and therefore the presence of $CD90^+$ cells in vivo cannot be ruled out. Such variation in immunostaining for HCC CSC is consistent with previous reports [46]. Nonetheless, given the localization of $CD44^+$ cells at the leading edge of the tumor, these findings raise the question, are $CD44^+$ HCC cells tumor propagating cells, and if so, do they promote local recurrence after an incomplete thermal ablation?

There are limitations to these studies. First, it is recognized that there are limitations in currently available techniques for identifying and studying CSC, including stem cell marker-based flow cytometry and immunohistochemistry [5, 46–48]. Second, the experiments were limited to one cell line. These findings warrant further validation not only in other HCC cell lines known to harbor $CD44^+$ and $CD90^+$ cells but also to other CSC markers in order to better understand the generalizability of these findings. Additionally, the mechanism or mechanisms whereby heat stress enriches the population of $CD44^+$ and $CD90^+$ cells warrants further investigation. Third, although $CD44^+$ and $CD90^+$ cells were identified in the N1S1 cell line and enriched by sublethal heat stress, these experiments do not confirm that these cells were in fact bona fide CSC. As such, $CD44^+$ and $CD90^+$ N1S1 HCC cells require further characterization using limiting dilution and serial transplantation assays in order to validate their role as CSC and determine whether they play a role in enhanced HCC tumorigenesis. Fourth, although these experiments suggest that PI3K-AKT-mTOR signaling may play a differential role in $CD44^+$ and $CD90^+$ HCC cellular response to heat stress, the cellular and molecular heterogeneity between $CD44^+$ and $CD90^+$ cells warrants further characterization in order to better understand the role of PI3K-AKT-mTOR in mediating cell proliferation and survival in these cellular subpopulations.

Residual HCC CSC within the thermal ablation zone represent a potential mechanism mediating recurrence and tumor progression to thermal ablative therapies for HCC. These studies provide experimental evidence supporting diverse roles for HCC cells expressing putative stem cell markers CD44 and CD90 in HCC biological response to heat stress. Given the enrichment of $CD44^+$ and $CD90^+$ cells after sublethal heat stress and the preferential localization of $CD44^+$ cells to tumor margin, these data may suggest that sublethal heat stress at the tumor ablation margin leaves behind residual $CD44^+$ and/or $CD90^+$ cells that can repopulate the tumor, thereby resulting in tumor relapse and progression. Of translational relevance, these data suggest that PI3K-mTOR may be a potential therapeutic target in $CD44^+$ and $CD90^+$ cells and support further studies investigating inhibition of the PI3K-AKT-mTOR pathway in combination with thermal ablation as a mechanism to sensitize potentially more refractory HCC subpopulations to heat stress. Although there is much more to be learned regarding the roles of $CD44^+$ and $CD90^+$ cells in HCC biological response to thermal ablation, these experiments suggest that the CSC hypothesis may be biologically and clinically relevant to the field of interventional oncology.

Acknowledgments

This publication was supported by CTSA Grant TL1 TR000137 from the National Center for Advancing Translational Science (NCATS). Additional research support provided in part by a SIR Foundation allied scientist training Grant. Infrastructure support was provided by NIH construction grant NIH C06 RR018898.

References

1. Jordan CT, Guzman ML, Noble M. Cancer stem cells. N Engl J Med. 2006; 355:1253–1261. [PubMed: 16990388]
2. Hamburger AW, Salmon SE. Primary bioassay of human tumor stem cells. Science. 1977; 197(4302):461–463. [PubMed: 560061]
3. Reya T, Morrison SJ, Clarke MF, Weissman IL. Stem cells, cancer, and cancer stem cells. Nature. 2001; 414(6859):105–111. [PubMed: 11689955]
4. Visvader JE, Lindeman GJ. Cancer stem cells in solid tumours: accumulating evidence and unresolved questions. Nat Rev Cancer. 2008; 8:755–768. [PubMed: 18784658]
5. Magee JA, Piskounova E, Morrison SJ. Cancer stem cells: impact, heterogeneity, and uncertainty. Cancer Cell. 2012; 21:283–296. [PubMed: 22439924]
6. Brabletz T. EMT and MET in metastasis: where are the cancer stem cells? Cancer Cell. 2012; 22:699–701. [PubMed: 23238008]
7. Park CY, Tseng D, Weissman IL. Cancer stem cell-directed therapies: recent data from the laboratory and clinic. Mol Ther. 2009; 17:219–230. [PubMed: 19066601]
8. Rosen JM, Jordan CT. The increasing complexity of the cancer stem cell paradigm. Science. 2009; 324(5935):1670–1673. [PubMed: 19556499]
9. Tong CM, Ma S, Guan XY. Biology of hepatic cancer stem cells. J Gastroenterol Hepatol. 2011; 26:1229–1237. [PubMed: 21557770]
10. Haraguchi N, Ishii H, Mimori K, et al. CD13 is a therapeutic target in human liver cancer stem cells. J Clin Investig. 2010; 120:3326–3339. [PubMed: 20697159]
11. Henry JC, Park JK, Jiang J, et al. miR-199a-3p targets CD44 and reduces proliferation of CD44 positive hepatocellular carcinoma cell lines. Biochem Biophys Res Commun. 2010; 403:120–125. [PubMed: 21055388]
12. Yang ZF, Ho DW, Ng MN, et al. Significance of $CD90^+$ cancer stem cells in human liver cancer. Cancer Cell. 2008; 13:153–166. [PubMed: 18242515]
13. Ma S, Lee TK, Zheng BJ, et al. $CD133^+$ HCC cancer stem cells confer chemoresistance by preferential expression of the Akt/PKB survival pathway. Oncogene. 2008; 27:1749–1758. [PubMed: 17891174]
14. Ma S, Chan KW, Lee TK, et al. Aldehyde dehydrogenase discriminates the CD133 liver cancer stem cell populations. Mol Cancer Res. 2008; 6:1146–1153. [PubMed: 18644979]
15. Yamashita T, Forgues M, Wang W, et al. EpCAM and alpha-fetoprotein expression defines novel prognostic subtypes of hepatocellular carcinoma. Cancer Res. 2008; 68:1451–1461. [PubMed: 18316609]
16. Terris B, Cavard C, Perret C. EpCAM, a new marker for cancer stem cells in hepatocellular carcinoma. J Hepatol. 2010; 52:280–281. [PubMed: 20006402]
17. Yoon SK. The biology of cancer stem cells and its clinical implication in hepatocellular carcinoma. Gut Liver. 2012; 6:29–40. [PubMed: 22375168]
18. Ji J, Wang XW. Clinical implications of cancer stem cell biology in hepatocellular carcinoma. Semin Oncol. 2012; 39:461–472. [PubMed: 22846863]
19. Rountree CB, Mishra L, Willenbring H. Stem cells in liver diseases and cancer: recent advances on the path to new therapies. Hepatology. 2012; 55:298–306. [PubMed: 22030746]
20. Colombo F, Baldan F, Mazzucchelli S, et al. Evidence of distinct tumour-propagating cell populations with different properties in primary human hepatocellular carcinoma. PLoS One. 2011; 6:e21369. [PubMed: 21731718]

21. Marquardt JU, Raggi C, Andersen JB, et al. Human hepatic cancer stem cells are characterized by common stemness traits and diverse oncogenic pathways. Hepatology. 2011; 54:1031–1042. [PubMed: 21618577]
22. Song K, Wu J, Jiang C. Dysregulation of signaling pathways and putative biomarkers in liver cancer stem cells [review]. Oncol Rep. 2013; 29:3–12. [PubMed: 23076400]
23. Chen X, Lingala S, Khoobyari S, et al. Epithelial mesenchymal transition and hedgehog signaling activation are associated with chemoresistance and invasion of hepatoma subpopulations. J Hepatol. 2011; 55:838–845. [PubMed: 21334406]
24. Lee TK, Castilho A, Ma S, Ng IO. Liver cancer stem cells: implications for a new therapeutic target. Liver Int. 2009; 29:955–965. [PubMed: 19490415]
25. Martelli AM, Evangelisti C, Follo MY, et al. Targeting the phosphatidylinositol 3-kinase/Akt/mammalian target of rapamycin signaling network in cancer stem cells. Curr Med Chem. 2011; 18:2715–2726. [PubMed: 21649579]
26. Dubrovska A, Kim S, Salamone RJ, et al. The role of PTEN/Akt/PI3K signaling in the maintenance and viability of prostate cancer stem-like cell populations. Proc Natl Acad Sci USA. 2009; 106:268–273. [PubMed: 19116269]
27. Sunayama J, Matsuda K, Sato A, et al. Crosstalk between the PI3K/mTOR and MEK/ERK pathways involved in the maintenance of self-renewal and tumorigenicity of glioblastoma stem-like cells. Stem Cells. 2010; 28:1930–1939. [PubMed: 20857497]
28. Xu Q, Simpson SE, Scialla TJ, et al. Survival of acute myeloid leukemia cells requires PI3 kinase activation. Blood. 2003; 102:972–980. [PubMed: 12702506]
29. Xu Q, Thompson JE, Carroll M. mTOR regulates cell survival after etoposide treatment in primary AML cells. Blood. 2005; 106:4261–4268. [PubMed: 16150937]
30. Hsu HS, Lin JH, Huang WC, et al. Chemoresistance of lung cancer stemlike cells depends on activation of Hsp27. Cancer. 2011; 117:1516–1528. [PubMed: 21425153]
31. Prinsloo E, Setati MM, Longshaw VM, Blatch GL. Chaperoning stem cells: a role for heat shock proteins in the modulation of stem cell self-renewal and differentiation? Bioessays. 2009; 31:370–377. [PubMed: 19274656]
32. Wright MH, Calcagno AM, Salcido CD, et al. Brca1 breast tumors contain distinct $CD44^{+}$ / $CD24^{-;}$ and $CD133^{+}$ cells with cancer stem cell characteristics. Breast Cancer Res. 2008; 10:R10. [PubMed: 18241344]
33. Lencioni R, Crocetti L. Local-regional treatment of hepatocellular carcinoma. Radiology. 2012; 262:43–58. [PubMed: 22190656]
34. Tiong L, Maddern GJ. Systematic review and meta-analysis of survival and disease recurrence after radiofrequency ablation for hepatocellular carcinoma. Br J Surg. 2011; 98:1210–1224. [PubMed: 21766289]
35. Wang JH, Wang CC, Hung CH, et al. Survival comparison between surgical resection and radiofrequency ablation for patients in BCLC very early/early stage hepatocellular carcinoma. J Hepatol. 2012; 56:412–418. [PubMed: 21756858]
36. Cho YK, Kim JK, Kim MY, et al. Systematic review of randomized trials for hepatocellular carcinoma treated with percutaneous ablation therapies. Hepatology. 2009; 49:453–459. [PubMed: 19065676]
37. Yin XY, Xie XY, Lu MD, et al. Percutaneous thermal ablation of medium and large hepatocellular carcinoma: long-term outcome and prognostic factors. Cancer. 2009; 115:1914–1923. [PubMed: 19241423]
38. Kao WY, Chiou YY, Hung HH, et al. Risk factors for long-term prognosis in hepatocellular carcinoma after radiofrequency ablation therapy: the clinical implication of aspartate amino-transferase–platelet ratio index. Eur J Gastroenterol Hepatol. 2011; 23:528–536. [PubMed: 21537128]
39. Ng KK, Poon RT, Lo CM, et al. Analysis of recurrence pattern and its influence on survival outcome after radiofrequency ablation of hepatocellular carcinoma. J Gastrointest Surg. 2008; 12:183–191. [PubMed: 17874276]
40. Liu Y, Zheng Y, Li S, et al. Percutaneous microwave ablation of larger hepatocellular carcinoma. Clin Radiol. 2013; 68:21–26. [PubMed: 22766484]

41. Thompson SM, Callstrom MR, Knudsen B, et al. Development and preliminary testing of a translational model of hepatocellular carcinoma for MR imaging and interventional oncologic investigations. J Vasc Interv Radiol. 2012; 23:385–395. [PubMed: 22265247]

42. Thompson SM, Callstrom MR, Knudsen B, et al. AS30D model of hepatocellular carcinoma: tumorigenicity and preliminary characterization by imaging, histopathology, and immunohistochemistry. Cardiovasc Intervent Radiol. 2013; 36:198–203. [PubMed: 22923329]

43. Yamashita T, Honda M, Nio K, et al. Oncostatin m renders epithelial cell adhesion molecule-positive liver cancer stem cells sensitive to 5-fluorouracil by inducing hepatocytic differentiation. Cancer Res. 2010; 70:4687–4697. [PubMed: 20484035]

44. Wang XQ, Ongkeko WM, Chen L, et al. Octamer 4 (Oct4) mediates chemotherapeutic drug resistance in liver cancer cells through a potential Oct4-AKT-ATP-binding cassette G2 pathway. Hepatology. 2010; 52:528–539. [PubMed: 20683952]

45. Cheung ST, Cheung PF, Cheng CK, et al. Granulin-epithelin precursor and ATP-dependent binding cassette (ABC)B5 regulate liver cancer cell chemoresistance. Gastroenterology. 2011; 140:344–355. [PubMed: 20682318]

46. Lingala S, Cui YY, Chen X, et al. Immunohistochemical staining of cancer stem cell markers in hepatocellular carcinoma. Exp Mol Pathol. 2010; 89:27–35. [PubMed: 20511115]

47. Hermansen SK, Christensen KG, Jensen SS, Kristensen BW. Inconsistent immunohistochemical expression patterns of four different CD133 antibody clones in glioblastoma. J Histochem Cytochem. 2011; 59:391–407. [PubMed: 21411810]

48. Mather JP. In vitro models. Stem Cells. 2012; 30:95–99. [PubMed: 22076915]

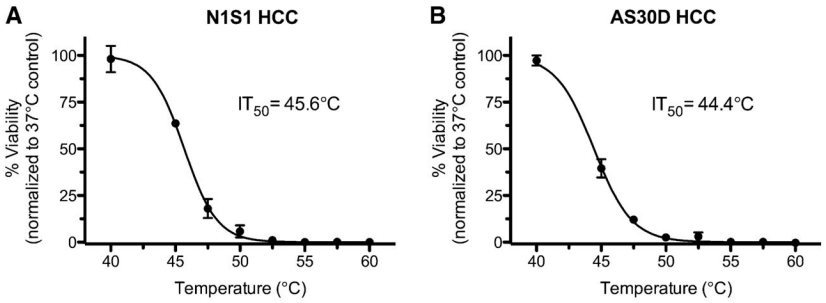

Fig. 1.

Effect of heat stress temperature on N1S1 and AS30D HCC cell viability. N1S1 and AS30D cells heat stressed at indicated temperatures from 37 to 60 °C for 10 min were assessed for viability with WST-1 assay at 48 h after heat stress. Data were normalized to 37 °C control and presented as mean ± SEM of 3 independent experiments. Nonlinear regression curve fitting was used to calculate heat stress IT_{50}. IT50 was defined as temperature that induces 50 %reduction in cell viability relative to 37 °C control for 10-min exposure time

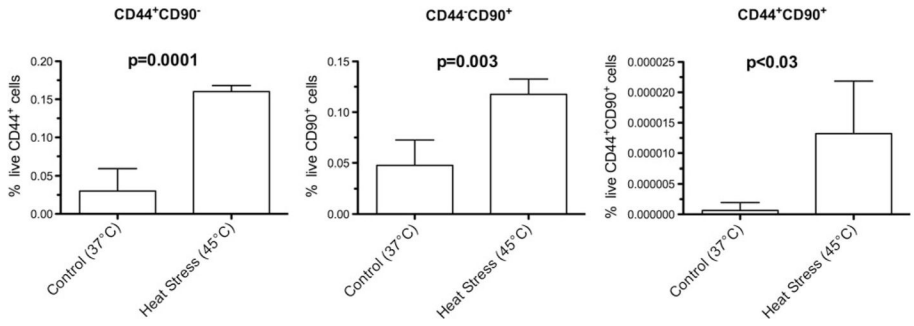

Fig. 2.

Effect of sublethal heat stress on proportion of live $CD44^+$, $CD90^+$, and $CD44^+$ $CD90^+$ N1S1 HCC cells. *Graph* shows that sublethal heat stress (45 °C, 10 min) resulted in significant increase in proportion of live $CD44^+$ $CD90^-$ (5.3-fold), $CD44^-CD90^+$ (2.4-fold), and $CD44^+$ $CD90^+$ (22.0-fold) N1S1 HCC cell subpopulations relative to control group (37 °C, 10 min) after 48-h recovery. Treatment groups compared by unpaired *t* test. Data are presented as mean ± SEM from 4 independent cell cultures

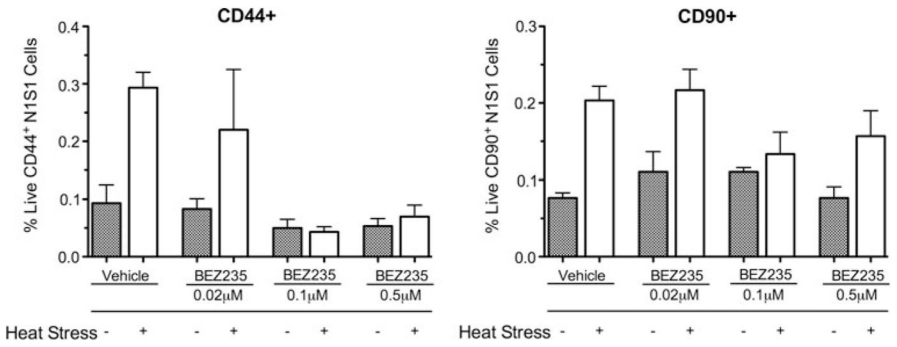

Fig. 3.

Effect of PI3K-mTOR inhibition on proportion of live $CD44^+$ and $CD90^+$ N1S1 HCC cells after sublethal heat stress. *Graph* shows that pretreatment with dual PI3K-mTOR inhibitor BEZ235 at 0.1 and 0.5 μM prevented heat stress-induced enrichment of population of live $CD44^+$ N1S1 cells after 48-h recovery ($p < 0.01$) but not $CD90^+$ N1S1 cells ($p > 0.10$). Treatment groups were compared by 1-way analysis of variance followed by post-hoc pairwise comparison by unpaired *t* test. Data are presented as mean ± SEM from 3 independent cell cultures

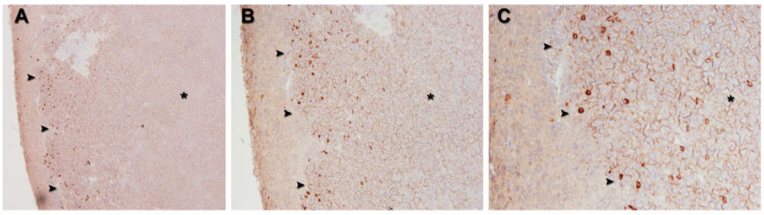

Fig. 4.

Representative CD44 immunostaining in orthotopic N1S1 HCC tumor model. **A** Low-power (50×), **B** medium-power (100×), and C high power (200×) photomicrographs of N1S1 tumors (*black asterisk*) demonstrate rare cells staining positive for CD44 (*brown*) preferentially localizing at tumor margin (*black arrowheads*) 24 h after sham ablation

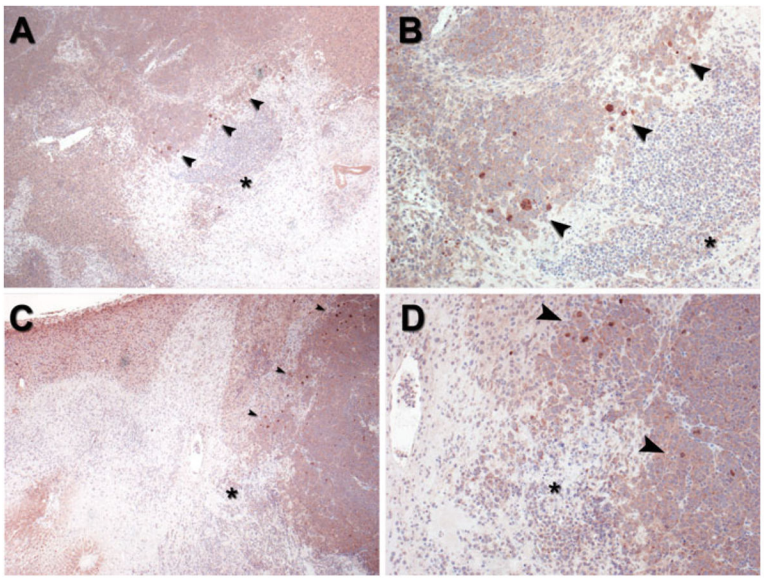

Fig. 5.

Representative CD44 immunostaining at tumor ablation margin in orthotopic N1S1 HCC tumor model from 2 different rats (**A**, **B** and **C**, **D**, respectively). **A**, **C** Low-power (40×) and **B**, **D** high-power (100×) photomicrographs of ablation zone (ablated tissue denoted by *black asterisk*) from both rats demonstrate clusters of rare cells staining positive for CD44 (*brown*) at tumor ablation margin (*black arrowheads*) 24 h after partial laser ablation